

New Method for Determining the Permeability Tensor of Magnetized Ferrites in a Wide Frequency Range

Patrick Quéffélec, *Member, IEEE*, Marcel Le Floch, and Philippe Gelin

Abstract—To provide a broad-band method for measuring the complex permeability tensor components of magnetized ferrites we have realized a nonreciprocal rectangular waveguide cell. A network analyzer setup is used to measure the scattering parameters of the cell over a wide range of frequencies. The nonreciprocity of the cell permits the determination of the permeability tensor components in a single experimental phase. Complex permittivity and complex components of the permeability tensor are computed from a data-processing program, taking into account higher order modes excited at the cell discontinuities and using a numerical optimization procedure to match calculated and measured values of the S -parameters. We have studied the convergence of the calculated S -parameters as the number of modes taken into account in the calculations. Sensitivity to the input parameters for the optimization algorithm is discussed. A thru-reflect-line calibration in conjunction with a specific sample holder is used to eliminate systematic errors inherent in the S -parameter measurements. Measured complex permeability tensor components data for microwave ferrites are presented at X -band frequencies (8–12 GHz). Experimental results are in good agreement with theoretical results given by the ferromagnetic material theory.

Index Terms—Anisotropic media, ferrites, inverse problem, microwave measurements, permeability measurement, waveguides.

I. INTRODUCTION

FERRITE materials are used in many microwave devices (circulators, phase shifters, tunable YIG filters, etc.) for their nonreciprocity due to the magnetic resonance and their low electrical conductivity that permits a strong interaction of the electromagnetic wave with the material in high frequencies. The microwave device is nonreciprocal when a static magnetic field H_o is applied to magnetize the ferrite sample. In this case, its permeability is a tensor quantity (anisotropic material) and depends on the signal frequency and magnitude of H_o . When H_o is applied along the y -axis, the permeability tensor in the Cartesian coordinate system takes the following well-known form:

$$\vec{\mu} = \begin{pmatrix} \mu^* & 0 & j\kappa^* \\ 0 & \mu_y^* & 0 \\ -j\kappa^* & 0 & \mu^* \end{pmatrix}$$

Manuscript received April 19, 1999.

P. Quéffélec and M. Le Floch are with the Laboratoire d'Electronique et Systèmes de Télécommunications, Unité Mixte de Recherche, Centre National de la Recherche Scientifique 6616, 29285 Brest Cedex, France, and are also with the Université de Bretagne Occidentale, Unité de Formation et de Recherche Sciences, 29285 Brest Cedex, France.

P. Gelin is with the Laboratoire d'Electronique et Systèmes de Télécommunications, UMR, Centre National de la Recherche Scientifique 6616, 9285 Brest Cedex, France, and is also with École Nationale Supérieure des Télécommunications de Bretagne, 29285 Brest Cedex, France.

Publisher Item Identifier S 0018-9480(00)06533-9.

where all tensor components $\mu^* = \mu' - j\mu''$, $\kappa^* = \kappa' - j\kappa''$, and $\mu_y^* = \mu_y' - j\mu_y''$ in a real medium are complex owing to the existence of magnetic losses.

In order to assist the microwave engineer in predicting the performance of nonreciprocal devices, the permeability of magnetized materials must be characterized. Until now, cavity resonator methods were used for measuring the permeability tensor components [1]. The resonant frequency and Q factor of a cavity resonator are measured with and without a suitably shaped specimen. In spite of its accuracy, the cavity method is applicable only over a narrow frequency band since measurements are limited by the cavity to fixed frequencies. Moreover, this method is not a suitable way of measuring high-loss materials, as the resonant frequency and Q factor measurement become less accurate, with consequent inaccuracy in the permittivity and permeability calculations in the vicinity of the magnetic resonance. Many researchers use the Weir method [2] to study the dynamic behavior of unsaturated ferrites over a wide range of frequencies. In this case, the measurements generally made in a coaxial line are wrong, for the theory used is based on a TEM calculation. This theory is no longer valid when the line contains an anisotropic material. Thus, the achievement of a broad-band measurement cell adapted to magnetized ferrites is needed.

We have first studied a microstrip line measurement cell developed in our laboratory for the broad-band characterization of isotropic materials [3]. The original feature of this method, in comparison with methods already existing [2], [4], lies in the fact that the sample under test is not machined to fit between the walls of the cell. This allows us to avoid practical mechanical difficulties, especially for ferrite materials, which may be fragile or granular in nature. However, this cell is reciprocal when containing a magnetized sample. In this case, the number of distinct measurements (the complex scattering parameters) is lower than the number of required parameters of the sample properties. Therefore, to measure the complex permeability tensor components of a magnetized ferrite, at least six independent measurements must be carried out.

We have then studied a rectangular waveguide measurement cell. The cell is nonreciprocal ($S_{21} \neq S_{12}$ and $S_{11} = S_{22}$) when the static magnetic field is applied along the small side of the waveguide and the sample does not entirely fill the waveguide section (Fig. 1). The nonreciprocity of the cell permits the measurement of the permeability tensor components in a single experimental phase. The data-processing program includes two calculation procedures. The first one is the electromagnetic analysis of the measurement cell that calculates the S -parameters as functions of the scalar permittivity $\epsilon^* = \epsilon' - j\epsilon''$, the permeability tensor $\vec{\mu}$, and dimensions of the ferrite

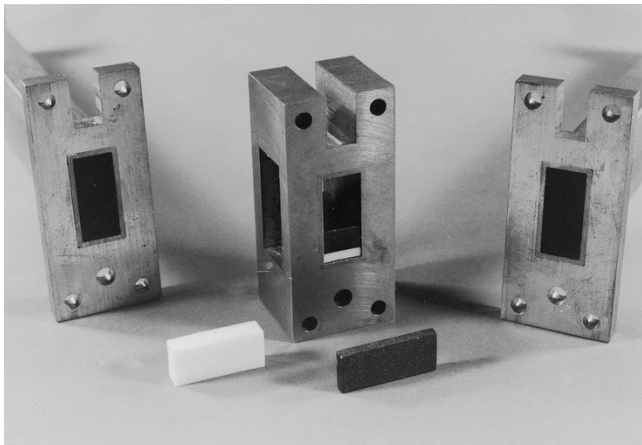


Fig. 1. Photograph of the rectangular waveguide measurement cell.

(direct problem). The second one is an optimization procedure that permits the determination of ϵ^* and $\vec{\mu}$ by matching the measured and calculated S -parameters (inverse problem).

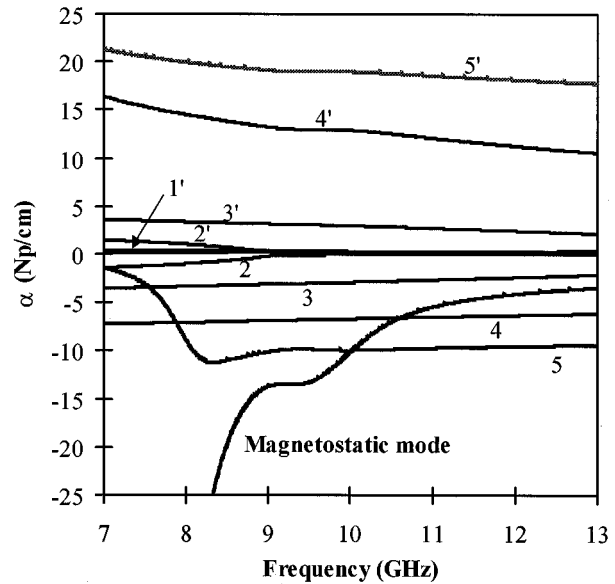
The purpose of this paper is not to describe the electromagnetic analysis of the cell thoroughly, as this has already been done in [5]. However, a brief recapitulation of its main features is necessary for a better understanding of the difficulties met in the inverse problem.

II. DIRECT PROBLEM

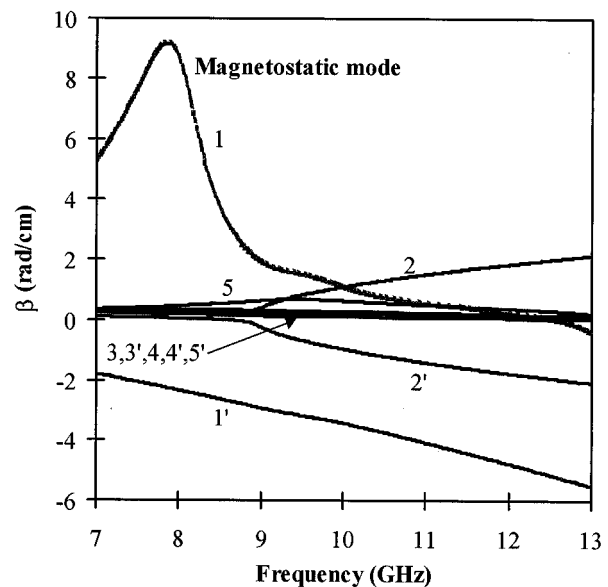
The electromagnetic analysis of the cell is based on the mode-matching method [6] applied to the waveguide discontinuities. This method requires the modes determination in the waveguide and the use of the orthogonality conditions between the modes.

A. Modal Analysis of the Cell

The main problem in the modal analysis is the calculation of the propagation constant for each mode in the waveguide partly filled with the ferrite. The modes are the complex roots of an eigenvalue equation containing poles [5]. The calculation procedure usually used for this kind of problem have proven to be ineffective in most cases. Thus, we had to realize a particular algorithm better adapted to the problem. The method is an extension to the complex plane of the dichotomic method. It consists in scanning a region of the complex plane with a square of small size to locate the point where the real and imaginary parts of the equation cancel each other simultaneously [5]. The algorithm has always shown a total reliability. It permits the accurate location of forward and backward modes of the cell whatever losses the ferrite may show. The algorithm also calculate the magnetostatic modes appearing in the cell. To illustrate the results given by the simulation software, Fig. 2 presents the evolution of the propagation constant of the first forward and backward modes of the waveguide versus frequency. We can notice on this graph that the waveguide containing an unsaturated ferrite propagates a magnetostatic mode whose group velocity is very low at 8 GHz (Fig. 2).



(a)



(b)

Fig. 2. Propagation constants $\gamma = \alpha + j\beta$ of the first forward and backward modes versus frequency. Waveguide dimensions: $a = 22.86$ mm, $b = 10.16$ mm. Ferrite parameters: thickness = 4 mm, $\epsilon^* = 14.5 - j0$, saturation magnetization $4\pi Ms = 5000$ G, anisotropy field $H_a = 180$ Oe, resonance linewidth $\Delta H = 500$ Oe. Dielectric parameters: thickness = 0.2 mm, $\epsilon^* = 1 - j0$ (air gap). 1: Forward dominant mode. 1': Backward dominant mode. 2-5: Forward higher order modes. 2-5': Backward higher order modes. (a) Attenuation constant α . (b) Phase constant β .

B. S-Parameters Calculation

The S -parameters of the cell are calculated from the continuity conditions on the fields at the unloaded/loading waveguide discontinuities (Fig. 3). The orthogonality of modes still holds even if the waveguide contains an anisotropic material [7]. The use of the orthogonality of modes enables us to determine the coupling coefficients ρ_n , T_i , R_r , and $t_n(n, i, r = 1, \dots, N)$ between modes from the continuity conditions on the fields [5],

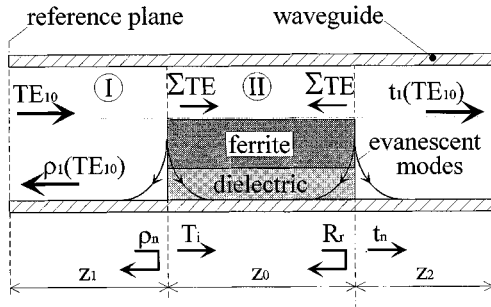


Fig. 3. Measurement cell discontinuities. Waveguide I: empty regions. Waveguide II: region partly filled with the ferrite.

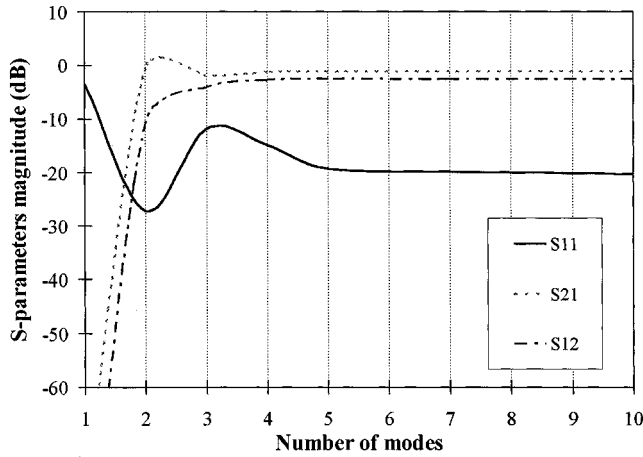


Fig. 4. Convergence of the S -parameters magnitude as the number of calculated modes. Frequency = 12 GHz.

where N is the number of modes taken into account in waveguides I and II (Fig. 3). Finally, the S -parameters of the cell are given by

$$\begin{aligned} S_{11} &= \rho_1 \exp(-2\gamma_1 z_1) \\ S_{12} &= t'_1 \exp(-\gamma_1(z_1 + z_2)) \\ S_{21} &= t_1 \exp(-\gamma_1(z_1 + z_2)) \\ S_{22} &= \rho'_1 \exp(-2\gamma_1 z_2) \end{aligned}$$

where γ_1 is the propagation constant of the dominant mode in waveguide I, ρ_1 and t_1 are the coupling coefficients between the forward dominant modes, and ρ'_1 and t'_1 are the coupling coefficients between the backward dominant modes. The S -parameters of the test device depend on the test material properties through the coefficients ρ_1 , t_1 , ρ'_1 , and t'_1 .

The rigorous description of the electromagnetic behavior of the cell requires to take an infinite number of modes into account in the calculation. In practice, the number of modes is fixed in such a way that the convergence of the calculated values of the S -parameters is obtained. We have studied the convergence of the S -parameters as the number of modes taken into account in each region of the waveguide. Fig. 4 shows that we can typically truncate the mode sums after about ten terms to obtain the accurate calculation of the S -parameters. Comparison between theoretical and experimental values of the S -parameters for ferrites of well-known properties in different magnetization

states have validated the electromagnetic analysis of the cell at X -band frequencies (8–12 GHz) [5].

III. INVERSE PROBLEM

From the given geometry of the ferrite and its position in the waveguide, the S -parameters are calculated using the previously described direct analysis for assumed values of the scalar permittivity and the permeability tensor components. This section presents computation of $\epsilon^* = \epsilon' - j\epsilon''$, $\mu^* = \mu' - j\mu''$, and $\kappa^* = \kappa' - j\kappa''$ of a given ferrite from the measured values of the S -parameters. The permeability component μ_y^* cannot be determined, as it does not appear in the S -parameters calculation, the modes being independent of the y variable [5].

A. Selection of the Optimization Method

Contrary to the case of the characterization methods for isotropic materials [2], [4], it is impossible here to express ϵ^* , μ^* , κ^* analytically according to the S -parameters since the electromagnetic analysis of the cell is complex. As a consequence, electromagnetic constants of a test sample are determined by matching calculated and measured values of the S -parameters using a numerical optimization procedure. An optimization problem involves minimizing a function, called the objective function, of several variables. The objective function can be expressed as a sum of squared functions as follows:

$$E(x) = \sum_{i=1}^2 \sum_{j=1}^2 |S_{ij\text{theoretical}}(x) - S_{ij\text{measured}}|^2 \quad (1)$$

where $x = (\epsilon', \epsilon'', \mu', \mu'', \kappa', \kappa'')$.

The optimization method is chosen in such a way that it permits a fast location of the global minimum of $E(x)$ by avoiding local minima.

The strong nonlinear character of the objective function, the presence of local minima, and the great number of variables led us to study optimization procedures of high performance. Among the algorithms we have programmed, two of them have proven to be superior. The first one is the More algorithm [8], which is an improvement of the Levenberg–Marquardt approach [9]. The second one is based on a sequential quadratic programming method [10]. The latter one is appropriate to calculate ϵ^* , μ^* , κ^* in a broad frequency band since the algorithm allows us to impose upper and lower bounds on all the variables. It permits to avoid the convergence of the calculations toward nonphysical solutions and to reduce the calculation time.

The most significant input parameters for optimization algorithms are the number of variables, initial estimate of the solution, and expression of the objective function. Sensitivity to these parameters for numerical results is discussed in the following section.

B. Input Parameters

The greater the number of variables is, the more difficult the location of the global minimum of the objective function is. Indeed, the number of alternative minima increases as the number of variables. In our case (six variables: ϵ' , ϵ'' , μ' , μ'' , κ' , κ''),

the convergence to the correct solution requires a reasonable initial guess. The determination of an approximate value of the solution is then necessary. It can be done using an analytical approach for the electromagnetic analysis of the cell or a physical model for the permeability tensor.

A quasi-static method can be used to describe the behavior of the cell in the case of a transmission line containing an isotropic material [2], [4]. This is unrealistic for a rectangular waveguide partly filled with an anisotropic ferrite.

The use of a physical model for the permeability tensor of unsaturated ferrites calls for the knowledge of many ferrite properties such as saturation magnetization, anisotropy field, resonance linewidth, and magnetization state. All these properties are not always given by the sample supplier. Moreover, the determination of the magnetization state of the material is very difficult in general.

In order to decrease the number of variables, the permittivity may be assumed to be independent of the static magnetic field H_o . This is a very realistic assumption for centimeter waves. When $H_o = 0$ Oe and the sample is completely demagnetized, the ferrite is an isotropic medium and by definition $\mu^* = \mu_y^*$ and $\kappa^* = 0$. The inverse problem is solved by assuming that the scalar permittivity ε^* and permeability μ^* are unknown and that the off-diagonal component κ^* vanishes. In a magnetized state, the ferrite is anisotropic and its permeability is a tensor quantity. The permittivity being known (measured ε^* data obtained for $H_o = 0$ Oe) resolution of the inverse problem gives us μ^* and κ^* . The problem is overdetermined since for six distinct measurements (S_{11} , S_{21} , and S_{12} magnitude and phase), there are four unknowns (μ' , μ'' , κ' , κ''). It allows us to avoid the determination of an approximate value of the correct solution of the inverse problem, numerical results being less dependent of the initial point. To make sure that this latter one is not too far from the correct solution, processing of the data begins at the highest frequency of the exploited frequency band. Indeed, in a completely demagnetized state of the ferrite or for ferrites with low anisotropy field, the magnetic resonance appears in the low frequency part of the centimeter waves range. In the experimental part of this paper, measurements are performed in X-band (8–12 GHz). Permeability tensor components may then be assumed to tend toward vacuum magnetic properties ($\mu' = 1$, $\mu'' = 0$, $\kappa' = 0$, $\kappa'' = 0$) at 12 GHz. For the starting frequency (12 GHz), iterations are confined within a region surrounding the value of the vacuum electromagnetic properties by imposing suitable bounds on the variables (initial value of each variable ± 10). At subsequent frequencies, the initial point is extrapolated using the values of ε' , ε'' , μ' , μ'' , κ' , and κ'' obtained at the previous frequencies. Iterations can then be confined within a small region around the initial point (initial value of each variable ± 0.1). The step frequency is less than 10^{-2} to make sure that extrapolated initial points are close enough to the correct solution of the inverse problem. Calculations are stopped when the lowest frequency (8 GHz) is reached.

Numerical results are very sensitive to the expression chosen to define the objective function. A great number of tests have shown that the objective function must be of a unit order in the investigated region to make the location of the correct solution easier. This condition depends on the expression of the objective

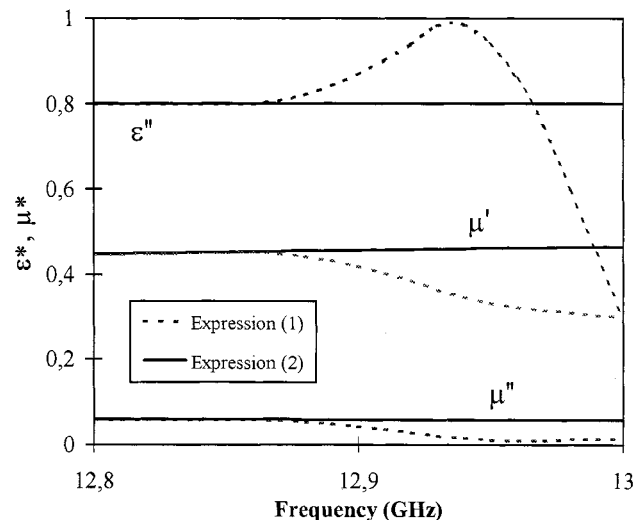


Fig. 5. Sensitivity to the expression of the objective function for the calculated values of ε'' , μ' , and μ'' .

function and the choice of the initial point. Many expressions have been studied for $E(x)$. Expression (1) has been chosen when the ferrite is magnetized. Paradoxically, when the material is completely demagnetized ($\kappa^* = 0 - j0$) the following form:

$$E(X) = \sum_{i=1}^2 \sum_{j=1}^2 \left| \frac{S_{ij}^{\text{theoretical}}(X)}{S_{ij}^{\text{measured}}} - 1 \right|^2 \quad (2)$$

greatly improves numerical results. This is confirmed by Fig. 5, where two different solutions are obtained using (1) and (2) for $E(x)$. Expression (2) permits the location of the correct solution over the entire frequency band, whereas the first one leads the numerical results toward an alternative minimum (nonphysical solution). The correct solution is subjected to physical constraints such as positive loss (μ'') over the full range of frequency and a typical variation in frequency of the gyrotropic resonance with the static magnetic field.

Finally, to give fast convergence, different iteration steps can be chosen for each variable. Iteration step is equal to 10^{-5} for ε' and ε'' and to 10^{-2} for μ' , μ'' , κ' , and κ'' . The typical central processing unit (CPU) time for 801 frequency points is less than 20 min using an IBM RS 6000 computer.

IV. EXPERIMENTS

A. Rectangular Waveguide Measurement System

Experiments are performed in X-band (8–12 GHz). Inside dimensions of the cross section of an X-band rectangular waveguide are 22.86×10.16 mm. The reflection and transmission coefficients of the X-band rectangular waveguide loaded with a ferrite sample are measured using an HP 8510 B network analyzer setup. Systematic errors due to the defects of the measurement cell (coaxial-to-waveguide adapters, copper losses of the conductors) and the network analyzer (coaxial cables, electronic components) can be reduced by a calibration procedure of the network analyzer. During the calibration, a series of known

devices (standards) are connected. The systematic errors are determined as the difference between the measured and known responses of the standards. Using the thru-reflect-line (TRL) calibration [11], the impedance mismatch at the coaxial-to-waveguide adapters can be characterized and removed. The TRL calibration relies on waveguides rather than on a set of discrete impedance standards. This procedure provides a direct waveguide interface. The calibration plane is established in the cell, near the ferrite. As a consequence, the S -parameters of the discontinuities created by the test sample in the waveguide can be measured directly. Moreover, the connection interface is repeatable since the same coaxial-to-waveguide adapters are used during the calibration process. This permits to obtain accurate measured ϵ^* , μ^* , and κ^* data.

In order to apply to the test sample static magnetic fields up to 20 kOe, the cell is set in between the poles of an electromagnet. To increase the cell sensitivity, the gyrotropic effect is intensified by setting the ferrite in a circularly polarized field area of the waveguide with a dielectric support (Fig. 1). The sample position in the waveguide and cell direction in the static magnetic field must be controlled to avoid additional systematic errors in the measured ϵ^* , μ^* , and κ^* data. This is obtained with a specific sample holder shown in Fig. 1. The sample holder has the same width as that of the electromagnet air gap to insure that the static field is applied along the small side of the rectangular waveguide. Moreover, the sample holder is not too long (length = 25 mm) for a better handling and insertion of samples in the cell. An additional length of waveguide (access waveguide) is inserted between the coaxial-to-waveguide adapters and sample holder. This is to insure that the higher order evanescent modes due to the coaxial-to-waveguide adapters are significantly attenuated prior reaching the test sample. During the calibration process, a short circuit is connected at the end of the access waveguide to each port. For the step "through," ports 1 and 2 of the network analyzer are connected with the two access waveguides. For the step "line," a short length of waveguide is inserted between the access waveguides. After the calibration process, the sample holder containing the test sample is inserted between the access waveguides using clamping screws and a metal rod to insure that the different waveguides are in a straight line. Finally, reference planes for S -parameter measurements are established in the access planes of the sample holder.

Ferrite samples of rectangular shape have the same width as that of the waveguide cross section (Fig. 1). Samples length must be less than those of the sample holder. Test samples have typical thickness of 2 mm. Sample dimensions are measured with a micrometer (accuracy = 1 μm). They are input parameters for the data-processing program. Due to inaccuracies in the machining of the test sample, air gaps may exist between the common surfaces of the ferrite material and waveguide. The presence of air gaps introduces errors in the estimation of ϵ^* , μ^* , and κ^* . In order to correct these errors, an air gap with a constant thickness equal to 50 μm has been introduced into the electromagnetic model of the cell [5]. Finally, the error arising

from uncertainty in the sample position in the cell can be corrected by using equations that are reference-plane invariant [12]

$$\begin{aligned} S_{21}^{\text{cor}} &= \frac{S_{21}}{S_{21}^o} \\ S_{12}^{\text{cor}} &= \frac{S_{12}}{S_{12}^o} \\ S_{11}^{\text{cor}} &= \frac{S_{11}S_{22}}{S_{21}S_{12}} \end{aligned}$$

where S_{ij}^{cor} , S_{ij} , and S_{ij}^o ($i, j = 1, 2$) are corrected, measured with the ferrite, and measured without the ferrite S -parameters, respectively.

B. Experimental Results

In this section, we present the measured permeability tensor components on two types of microwave ferrites in different magnetization states to validate the present method. Fig. 6 shows for different values of the static magnetic field H_o , typical measured μ^* and κ^* data versus frequency for a microwave ferrite of saturation magnetization $4\pi M_s = 5000$ G. The measured μ^* and κ^* data are obtained by starting from the zero field for a completely demagnetized sample. When the sample is demagnetized ($H_o = 0$ Oe), ferromagnetic material theory predicts that the magnetic resonance extends up to the frequency corresponding to the highest possible value of the demagnetizing field in the sample $f_{\text{max}} = \gamma 4\pi M_s = 14$ GHz, where γ is the gyromagnetic ratio and $\gamma = 2.8$ GHz/kOe. This is confirmed by the measured μ^* spectrum of the test sample [see Fig. 6(a)]. Indeed, in Fig. 6(a), it is seen that upper frequencies for the loss region are greater than 11.5 GHz. Moreover, we can notice that, at 0 Oe, the real and imaginary part of the off-diagonal component κ^* are zero. The nonzero value of κ^* in partly magnetized states ($H_o \neq 0$ Oe) prove the anisotropy and nonreciprocity characters of the test sample [see Fig. 6(b)–(d)]. Above 500 Oe, the magnetic resonance appears at X-band frequencies [see Fig. 6(c) and (d)]. Imaginary parts μ'' and κ'' of the permeability tensor components exhibit a rather well-resolved peak due to the damped precession of the spins around the external magnetic field H_o . The variation in frequency of the magnetic resonance for the measured κ'' spectrum is shown in Fig. 7. This is a typical variation predicted by the well-known theoretical law

$$\Delta f_r = \gamma \Delta H_o$$

where Δf_r is the shift of the magnetic resonance frequency and ΔH_o is the strength variation of the static magnetic field. This relation predicts a linear dependence of Δf_r with ΔH_o , which is actually observed in Fig. 7. Indeed, it can be seen from the figure that the measured frequency corresponding to the maximum of permeability loss is tuned magnetically from 8.26 to 9.67 GHz for $\Delta H_o = 500$ Oe. Theoretical ($\gamma \Delta H_o = 1.40$ GHz) and measured ($\Delta f_r = 1.41$ GHz) values for the variation in frequency of f_r are in close agreement. We can also notice in Fig. 7 that, as would be expected, the half-bandwidth of the loss component κ'' is sharper when H_o is increasing. Moreover, negative values for κ'' are obtained when $H_o = 250$ Oe. This result has already

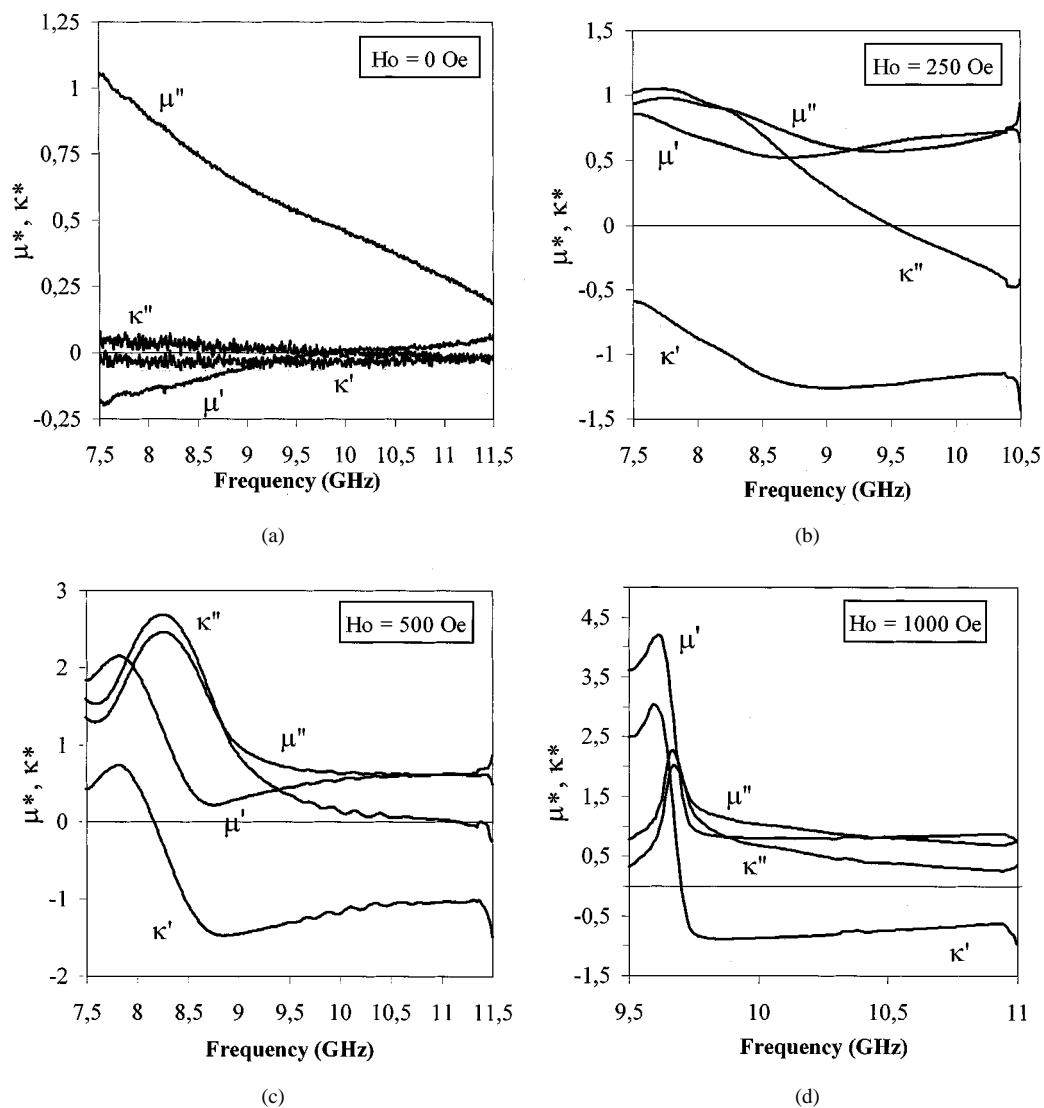


Fig. 6. Measured μ^* and κ^* data versus frequency for different values of the static magnetic field H_o . Ferrite under test properties: $4\pi M_s = 5000$ G, $H_a = 200$ Oe, and $\Delta H = 500$ Oe. (a) Magnetic static field applied $H_o = 0$ Oe. (b) Magnetic static field applied $H_o = 250$ Oe. (c) Magnetic static field applied $H_o = 500$ Oe. (d) Magnetic static field applied $H_o = 1000$ Oe.

been measured in [13] using a cavity resonator method out of the loss region. All these experimental results confirm the validity of the broad-band method we have worked out.

Due to the sample length (length = 20 mm), singular points (dimensional resonance) appear in the measured scattering parameter S_{11} at X-band frequencies. At frequencies corresponding to integer multiples of one-half wavelength S_{11} magnitude gets very small with consequent large phase uncertainty. The correct solution of the inverse problem is divergent making the location of the global minimum difficult. That is why μ^* and κ^* calculations are stopped at 9.5 GHz when $H_o = 1$ kOe [see Fig. 6(d)]. For a microwave ferrite of saturation magnetization $4\pi M_s = 2386$ G, measured μ^* and κ^* data versus frequency exhibit a dimensional resonance at 9.9 GHz when $H_o = 4.5$ kOe (Fig. 8). To bypass this problem, samples which are less than one half-wave long at the highest measurement frequency can be used. However, the use of short samples decreases measurement accuracy. To avoid this drawback, we plan on using a different approach for the resolu-

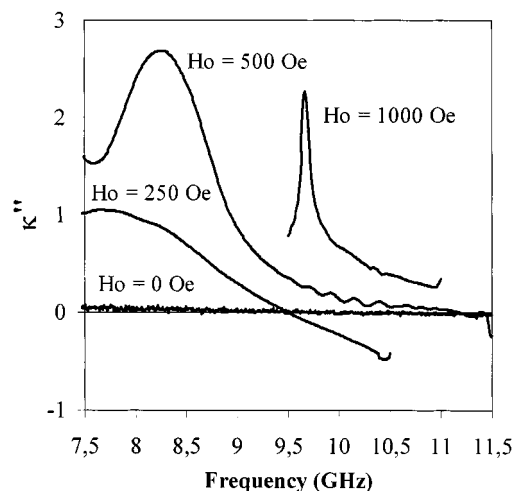


Fig. 7. Variation in frequency of the magnetic resonance for the measured κ'' spectrum.

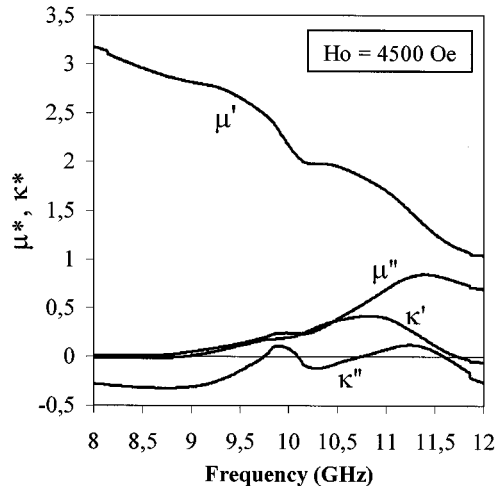


Fig. 8. Measured μ^* and κ^* data versus frequency for $H_o = 4.5$ kOe. Ferrite under test properties: $4\pi Ms = 2386$ G.

tion of the inverse problem. This approach has been proposed by Baker-Jarvis *et al.* [14]. It consists of solving the inverse problem over the entire frequency range using S -parameters magnitude alone. Magnitude data have the advantage of being independent of dimensional resonance problems. The variables of the inverse problem are not ε^* , μ^* , and κ^* anymore, but the coefficients of an explicit frequency-dependent form for ε^* , μ^* , and κ^* . The Debye model can be used to describe the variation in frequency of permittivity

$$\varepsilon^* = \frac{A}{1 + jB\omega} + C$$

where ω is the angular frequency and A , B , and C are variables of the inverse problem. However, to apply this approach to the characterization of magnetized ferrites, analytical functions for μ^* and κ^* must be studied.

V. CONCLUSION

We have worked out a data-processing program in conjunction with a rectangular waveguide cell permitting the broad-band determination of the permeability tensor of magnetized ferrites. The method is easy to use and enables the broad-band determination of the diagonal and off-diagonal components of the permeability tensor in a single experimental phase. In the direct analysis, higher order modes and especially magnetostatic modes are taken into account for a thorough description of the dynamic behavior of the nonreciprocal cell. Magnetic losses are also accessible thanks to the development of a well-performing complex root-finding technique. A sequential quadratic programming method is used to determine the complex permittivity and the complex permeability tensor components of magnetized ferrites by matching the calculated value with the measured value of the scattering parameters of the cell. The measured μ^* and κ^* obtained at X -band frequencies using a specific sample holder and the TRL calibration are in good agreement with theoretical results predicted by the ferromagnetic material theory. Moreover, the method can be extended to upper or lower frequency ranges using the

same data-processing program and rectangular waveguides of different dimensions.

REFERENCES

- [1] J. Krupka, "Measurements of all complex permeability tensor components and the effective line widths of microwave ferrites using dielectric ring resonators," *IEEE Trans. Microwave Theory Tech.*, vol. 39, pp. 1148–1157, July 1991.
- [2] W. B. Weir, "Automatic measurement of complex dielectric constants and permeability at microwave frequencies," *Proc. IEEE*, vol. 62, pp. 33–36, Jan. 1974.
- [3] P. Quéffélec, P. Gelin, J. Gieraltowski, and J. Loaëc, "A microstrip device for the broad-band simultaneous measurement of complex permeability and permittivity," *IEEE Trans. Magn.*, vol. 30, pp. 224–231, Mar. 1994.
- [4] W. Barry, "A broad-band automated stripline technique for the simultaneous measurement of complex permittivity and permeability," *IEEE Trans. Microwave Theory Tech.*, vol. MTT-34, pp. 80–84, Jan. 1986.
- [5] P. Quéffélec, M. Le Floch, and P. Gelin, "Nonreciprocal cell for the broad-band measurement of tensorial permeability of magnetized ferrites: Direct problem," *IEEE Trans. Microwave Theory Tech.*, vol. 47, pp. 390–397, Apr. 1999.
- [6] J. Esteban and J. M. Rebolgar, "Characterization of corrugated waveguides by modal analysis," *IEEE Trans. Microwave Theory Tech.*, vol. 39, pp. 937–943, June 1991.
- [7] S. W. Yun, M. J. Lee, and I. S. Chang, "Analysis of step discontinuities on planar dielectric waveguide containing a gyrotropic layer," *IEEE Trans. Microwave Theory Tech.*, vol. 37, pp. 492–495, Mar. 1989.
- [8] J. J. More, *The Levenberg-Marquardt Algorithm: Implementation and Theory*. Berlin, Germany: Springer-Verlag, 1978.
- [9] D. W. Marquardt, "An algorithm for least squares estimation of nonlinear parameters," *SIAM J. Appl. Math.*, vol. 11, pp. 431–441, 1963.
- [10] P. E. Gill, W. Murray, and M. H. Wright, *Practical Optimization*. New York: Academic, 1981.
- [11] G. Engen and C. Hoer, "Thru-reflect-line: An improved technique for calibrating the dual six-port automatic network analyzer," *IEEE Trans. Microwave Theory Tech.*, vol. MTT-27, pp. 987–993, Dec. 1979.
- [12] J. Baker-Jarvis, E. J. Venzura, and W. A. Kissick, "Improved technique for determining complex permittivity with the transmission/reflection method," *IEEE Trans. Microwave Theory Tech.*, vol. 38, pp. 1096–1103, Aug. 1990.
- [13] R. C. Le Craw and E. G. Spencer, "Tensor permeabilities of ferrites below magnetic saturation," in *IRE Conv. Rec. Pt. 5*, New York, 1956, pp. 66–74.
- [14] J. Baker-Jarvis, R. G. Geyer, and P. D. Domich, "A nonlinear least-squares solution with causality constraints applied to the transmission line permittivity and permeability determination," *IEEE Trans. Microwave Theory Tech.*, vol. 41, pp. 646–652, May 1992.



Patrick Quéffélec was born in France, in 1966. He received the Ph.D. degree in electronics from the University of Brest, Brest, France, in 1994.

He is currently a Maître de Conférences in the Laboratoire d'Electronique et Systèmes de Télécommunications, Unité Mixte de Recherche, Centre National de la Recherche Scientifique 6616, University of Brest. His research activities deal with the electromagnetic-wave propagation in heterogeneous materials and the analysis of measurement methods for the microwave characterization of materials.



Marcel Le Floch was born in France, in 1945. He received the Docteur-ès-Sciences degree from the Université de Bretagne Occidentale, Brest, France, in 1983.

He is currently a Professor in the Electronic Department, Université de Bretagne Occidentale. He is also a member of the Laboratoire d'Electronique et Systèmes de Télécommunications, Unité Mixte de Recherche, Centre National de la Recherche Scientifique 6616, University of Brest.



Philippe Gelin was born in France, in 1948. He received the Ph.D. degree in physics from the Technical University of Lille, Lille, France, in 1981.

He is currently a Professor of electrical engineering at the Ecole Nationale Supérieure des Télécommunications de Bretagne, Brest, France. His research interests include wave-matter interactions and the modeling and the characterization of materials. He is a member of the Laboratoire d'Electronique et Systèmes de Télécommunications, which is a research unit associated with the French

National Research Council Unité Mixte de Recherche, Centre National de la Recherche Scientifique 6616, University of Brest, Brest, France.